#### **NURETH14-436**

# DEVELOPMENT OF DIRECT STEAM-WATER PHASE CHANGE ANALYSIS METHOD APPLYING TO BWR OPERATING CONDITION

### M. Fukuta, Y. Yamamoto and T. Mitsutake

Toshiba Corporation, 8 Sinsugita-Cho, Isogo-Ku, Yokohama, Japan masato.fukuta@toshiba.co.jp, yasushi3.yamamoto@toshiba.co.jp, tooru.mitsutake@toshiba.co.jp

#### **Abstract**

A simulation method applicable to estimation of the two-phase flow in Next Generation BWR fuel assembly has been developed. In this paper, to realize "design-by-analysis", two CFD analysis models were developed. Firstly, the hybrid two-phase flow analysis model was developed to simulate the flow pattern transition. Using this model, it was confirmed that the generation of large bubbles by bubble coalescence could be simulated. Secondly, to analyze boiling phenomena, a phase-field model combined with Navier-Stokes equations was developed. We succeeded in simulating the boiling process, bubble nucleation, growth, and departure from heating wall directly under the BWR in-core pressure condition.

#### Introduction

In the nuclear reactor core development for future BWR, it is important that the boiling two-phase flow phenomena is comprehended and evaluated in detail. Yamamoto et al. [1] developed the design procedure called Practical Design-by-Analysis (PDBA) method to realize the large size bundle design for the future reactor. In this procedure, the partial mock-up test and numerical analysis are consisted shown in Figure 1. For the numerical analysis in PDBA, the subchannel analysis method is included to evaluate the two-phase flow behaviour in a subchannel. The input data such as the space effect model coefficient and the critical power correlation is evaluated with the partial mockup experimental data. Next, the critical power of the full-bundle size is evaluated by the subchannel analysis and the critical power correlation is improved based on the subchannel analysis result. In this PDBA method, the mock-up test is needed and the local two-phase flow phenomena can not be understood because of the difficulty to obtain the local unsteady data by experiment. On the other hand, there is another design procedure method called Full Design-by-Analysis (FDBA) [2], which consists of the subchannel analysis and Computational Fluid Dynamics (CFD). In CFD code, for example, the Euler-Lagrange method, Volume of Fluid (VOF) method, Lattice Boltzmann method (LBM), Two Fluid (TF) model and Moving Particle Semi-implicit (MPS) method are used for estimate the two-phase phenomena. These CFD methods are applied to predict the local small scale two-phase phenomena in a fuel bundle such as the void drift between the subchannels or the spacer effect. By constructing the FDBA method, the mechanistic modelling for the two-phase phenomena seems to be realized. To development of the FDBA, two new two-phase CFD analysis methods are developed in this paper for evaluating the two-phase flow pattern transition, and the boiling phenomenon directly, the hybrid two-phase flow analysis model and the boiling simulation method by Phase-Field model. These two numerical analysis methods are explained and the simulation results are represented in the following chapters.

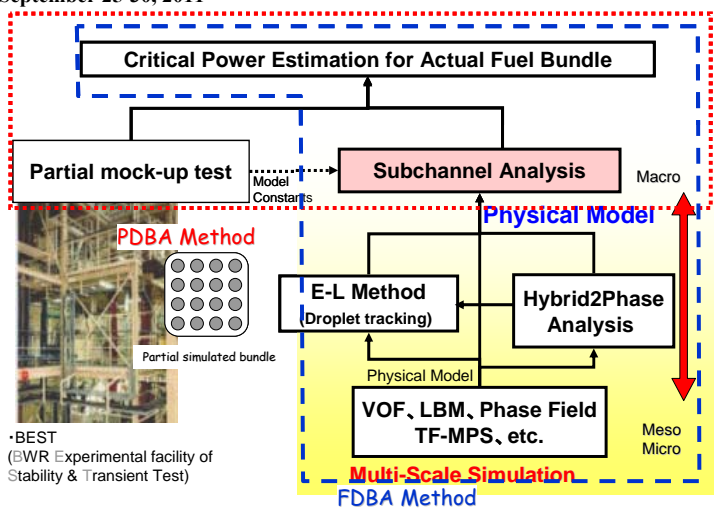


Figure 1 Schematic image of design by analysis.

# 1. Hybrid two-phase flow analysis model

To evaluate the complex two-phase flow phenomena such as a flow pattern transition in detail, or a void drift between sub-channels, it is important that various size bubbles behaviour is estimated simultaneously. Previous two-phase analysis methods are difficult to meet this requirement because each analysis method is limited the range of application about a bubble size. For example, VOF method can calculate the large bubble deformation or film flow behaviour, but when VOF method applied to the bubbly flow which contains many small bubbles ( $d \le O(1)$ mm), the computational cost becomes unrealistically large. In contrast, the Eulerian two-fluid model can be applied to a flow with many bubbles, for this model treats bubbles existing as void fraction. However, the Eulerian two-fluid model can not calculate the steam-water interface behaviour directly and uses the constitutive equations and empirical laws for evaluating this behaviour. For these reasons, it is needed that a new two-phase flow analysis method is developed which can evaluate a flow pattern transition in BWR sub-channels.

To meet these need, we developed a "hybrid two-phase flow analysis model" by coupling the VOF method and two-fluid model [3][4]. In this model, the gas-liquid interface behaviour of large bubbles or liquid films is calculated by VOF method, and a number of small bubbles behaviours are calculated by two-fluid model as shown in Figure 2. This hybrid model can calculate the two-phase flow consisting of various size bubbles and liquid film effectively. In addition, the bubble coalescence model was implemented in the present model. This model can estimate the coalescence of small bubbles and growth to large bubbles by switching the analysis method from two-fluid model to VOF method.

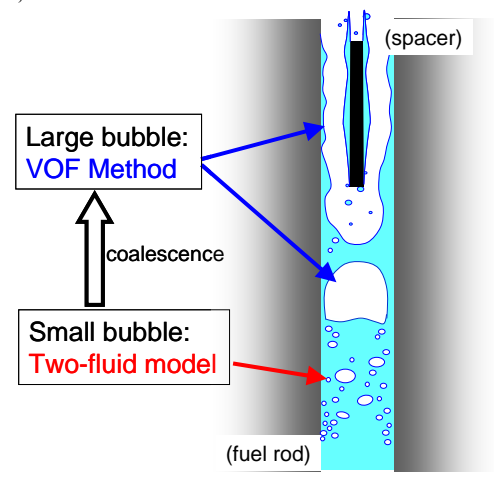


Figure 2 Schematic image of hybrid model for two-phase flow in BWR fuel sub-channel.

# 1.1 Governing equations and numerical method

Governing equations for hybrid two-phase flow analysis model are as bellows but only under the isothermal condition.

Mass conservation equations: 
$$\frac{\partial}{\partial t} (\alpha_{VOF} \rho_{VOF}) + \nabla \cdot (\alpha_{VOF} \rho_{VOF} \mathbf{u}) = \Gamma$$
 (1)

$$\frac{\partial}{\partial t} (\alpha_b \rho_b) + \nabla \cdot (\alpha_b \rho_b \mathbf{u}_b) = -\Gamma \tag{2}$$

Momentum conservation equations:

$$\frac{\partial}{\partial t} (\alpha_{VOF} \rho_{VOF} \mathbf{u}) + \nabla \cdot (\alpha_{VOF} \rho_{VOF} \mathbf{u} \mathbf{u}) 
= -\alpha_{VOF} \nabla p + \nabla \cdot (\alpha_{VOF} \tau) + \alpha_{VOF} \rho_{VOF} \mathbf{g} + \mathbf{F}_{VOF} + \mathbf{F}_{ST} + \Gamma \mathbf{u}_{b}$$
(3)

$$\frac{\partial}{\partial t} (\alpha_b \rho_b \mathbf{u}_b) + \nabla \cdot (\alpha_b \rho_b \mathbf{u}_b \mathbf{u}_b) = -\alpha \nabla p + \nabla (\alpha_b \tau_b) + \alpha_b \rho_b \mathbf{g} + \mathbf{F}_{ib} - \Gamma \mathbf{u}_b$$
(4)

In these equations,  $\alpha$ ,  $\rho$ ,  $\mathbf{u}$  and  $\tau$  are the volume fraction, density, velocity vector and viscous stress. Index VOF represents the value for the liquid and large bubble phase (VOF phase), and index b for the small bubble phase.  $\Gamma$  is the rate of production of VOF phase mass from the small bubble phase caused by bubble coalescences.  $\mathbf{F}_{VOF}$  and  $\mathbf{F}_{ib}$  are the interfacial friction ( $\mathbf{F}_{VOF} = -\mathbf{F}_{ib}$ ), and  $\mathbf{g}$  represents the gravity acceleration. For simulation of the gas-liquid interface behavior, VOF equation is calculated as shown below.

VOF equation: 
$$\frac{\partial}{\partial t} (\alpha_{VOF} \alpha_L) + \alpha_{VOF} \mathbf{u} \cdot \nabla \alpha_L = 0$$
 (5)

 $\alpha_L$  is the volume fraction of the liquid phase in the VOF phase. When the volume fraction of the gas phase inside of large bubbles in the VOF phase is represented by  $\alpha_G$ , the relation shown in Equation (6) can be satisfied between the volume fractions for each phase.

$$\alpha_b + \alpha_{VOF}\alpha_G + \alpha_{VOF}\alpha_L = \alpha_b + \alpha_{VOF}(\alpha_G + \alpha_L) = \alpha_b + \alpha_{VOF} = 1$$
 (6)

In this paper, the drag and lift forces are considered for the interface friction on the small bubble phase and this is solved by Equation (7).

$$\mathbf{F}_{ib} = \frac{3}{4} \frac{\alpha_b \rho_L C_D}{D} |\mathbf{u} - \mathbf{u}_b| (\mathbf{u} - \mathbf{u}_b) + \alpha_b \rho_L C_L (\mathbf{u}_b - \mathbf{u}) \times (\nabla \times \mathbf{u}) = -\mathbf{F}_{VOF}$$
(7)

 $C_D$  is the drag coefficients for a single bubble rising in water. For calculating  $C_D$ , the empirical correlation of Wang [5] is used as Equation (8).

$$C_D = \exp\left[a + b \ln Re_b + c(\ln Re_b)^2\right] \quad Re_b = \frac{\rho_L |\mathbf{u} - \mathbf{u}_b| D_b}{\mu_L}$$
(8)

 $Re_b$  is bubble Reynolds number and  $D_b$  is a bubble diameter. Coefficients a, b and c of Equation (8) are given in Table 1.

$Re_b$	а	b	c
$Re_b \le 1$	ln 16	-1	0
$1 < Re_b \le 450$	2.699467	-0.33581596	-0.07135617
$450 < Re_b \le 4000$	-51.77171	13.1670725	-0.8235592
$Re_b > 4000$	ln (8/3)	0	0

Table 1 Coefficients of Wang's drag correlation.

And  $C_L$  is the lift coefficient of a single bubble in a shear flow. For a spherical bubble in a weakly rotational inviscid flow,  $C_L = 0.5$  which derived by Auton [6] theoretically and this value was used in this paper.

In VOF phase, it is important that the surface tension is considered to predict the large bubble deformation. The CSF (Continuum Surface Force) model [7], which calculates the surface tension with Equation (9), is applied to the present model,

$$\mathbf{F}_{ST} = \alpha_{VOF} \sigma \kappa \frac{\mathbf{n}}{|\mathbf{n}|} = \alpha_{VOF} \sigma \kappa \nabla \alpha_L \frac{\rho_{VOF}}{\rho_m}$$
(9)

where  $\sigma$ ,  $\kappa$  and **n** are the surface tension coefficient, the local curvature of the bubble surface and the normal vector at the interface. The curvature is calculated by Equation (10).

$$\kappa = \frac{1}{|\mathbf{n}|} \left[ \left( \frac{\mathbf{n}}{|\mathbf{n}|} \cdot \nabla \right) |\mathbf{n}| - (\nabla \cdot \mathbf{n}) \right], \quad \mathbf{n} = \nabla \alpha_L$$
 (10)

In terms of the bubbles coalescences, the present model simulates it by switching the analysis method from two-fluid model to VOF method when a local flow field satisfies one condition. In this paper, the volume fraction value of each phase is used for the bubble coalescence condition as shown in Equation (11),

$$\frac{\alpha_b}{\alpha_b + \alpha_L \cdot (1 - \alpha_b)} > \alpha_{\text{max}} \tag{11}$$

where  $\alpha_{max}$  represents the threshold of the volume fraction. The coalescence is assumed to occur when Equation (11) is satisfied, and the coalescence is evaluated by converting  $\alpha_b$  to  $\alpha_{VOF}$   $\alpha_G$  as shown in Figure 3. In this paper, for development of the present CFD code, "The multi physics flow simulation system FrontFlow/red [8]" was used as the base program and the hybrid two-phase flow analysis model was implemented.

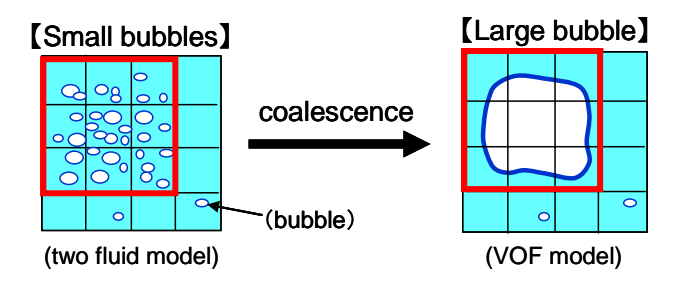


Figure 3 Image of bubble coalescence model for the hybrid simulation.

#### 1.2 Results and discussions

By developing simulation method, we calculated two problems for testing the effect of hybrid analysis. First, we calculated a large rising bubble in stationary two-phase flows containing small bubbles in a horizontal pipe. The three dimensional computational domain is shown in Figure 4. The gas phase is air and the liquid phase is water at the atmospheric pressure. The bubble diameter of the small bubbles is constant 0.1mm. For initial condition, the high void fraction region ( $\alpha_b = 0.9$ ), which is dealt as the small bubbles phase by the Eulerian two-fluid model, is set at the lower region in a pipe. Figure 5 represents the void fraction distribution around a large bubble rising in a pipe calculated by the present hybrid method at each time. It is found that the bubble coalescence is occurred at the high void fraction region, and single large bubble formed by the present coalescence model soon after the start of the calculation. After that, the large bubble rises with deforming into the spherical cap shape, and the low void fraction region is formed in the downstream region of a large bubble. From these results, it is confirmed that the present method can predict the small bubbles behaviour and the large bubbles deformation simultaneously.

Secondly, we applied the hybrid method to the upward two-phase flow problem. The computational domain is illustrated in Figure 6. The domain is two dimensional and the two-phase flow in the parallel flat plate is simulated. The domain size is 60mm x 1.0m. The uniform flow, whose void

fraction is 0.5, is given as the boundary condition at the lower inlet, and the free outflow is given as upper boundary condition. The small bubbles size is 4.0mm in this case. Figure 7 shows the time progression of the void fraction distribution obtained by the present method. It is found that the high void fraction region is being formed in a flow as the time progresses. This represents that the small bubbles migrate toward the wall and the high void fraction region forms near the wall. When the local void fraction satisfies the condition as Equation (11), the small bubbles coalesce and become large bubbles. By the present bubble coalescence model, it was confirmed that the two-phase flow developing and the appearance of the intermittent flow can be predicted.

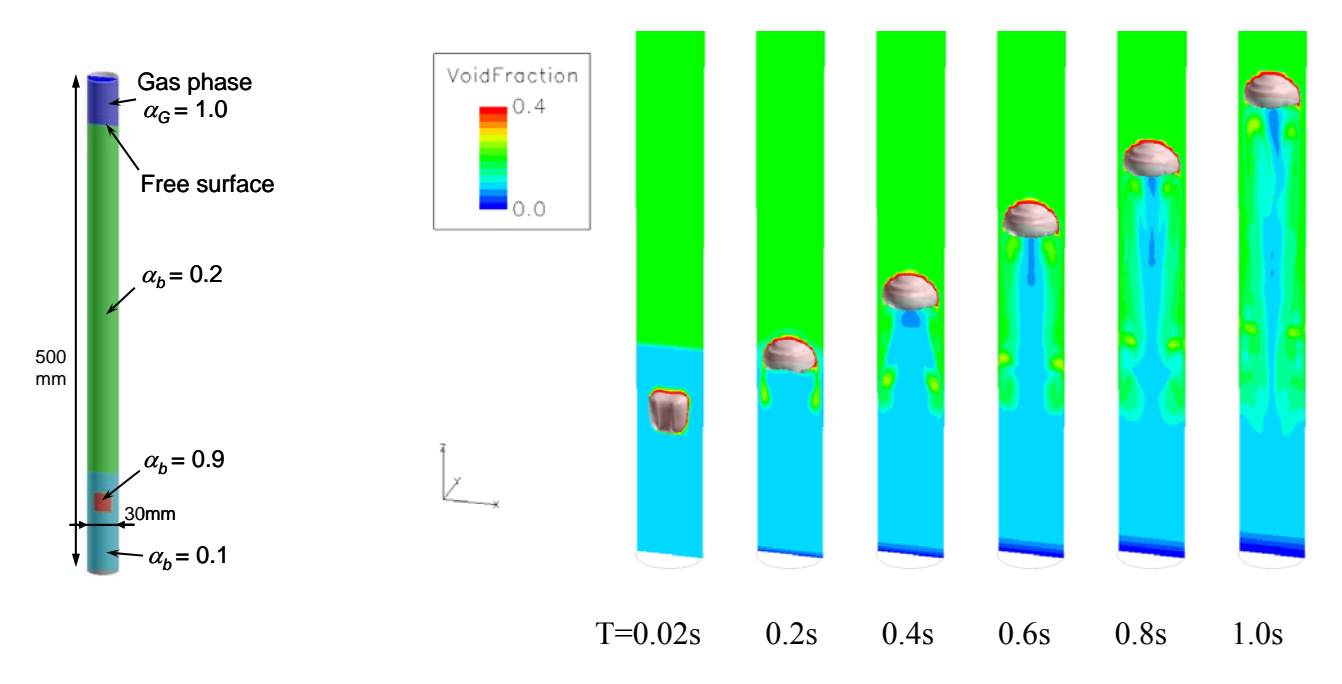


Figure 4 Computational domain.

Figure 5 Void fraction around a large bubble.

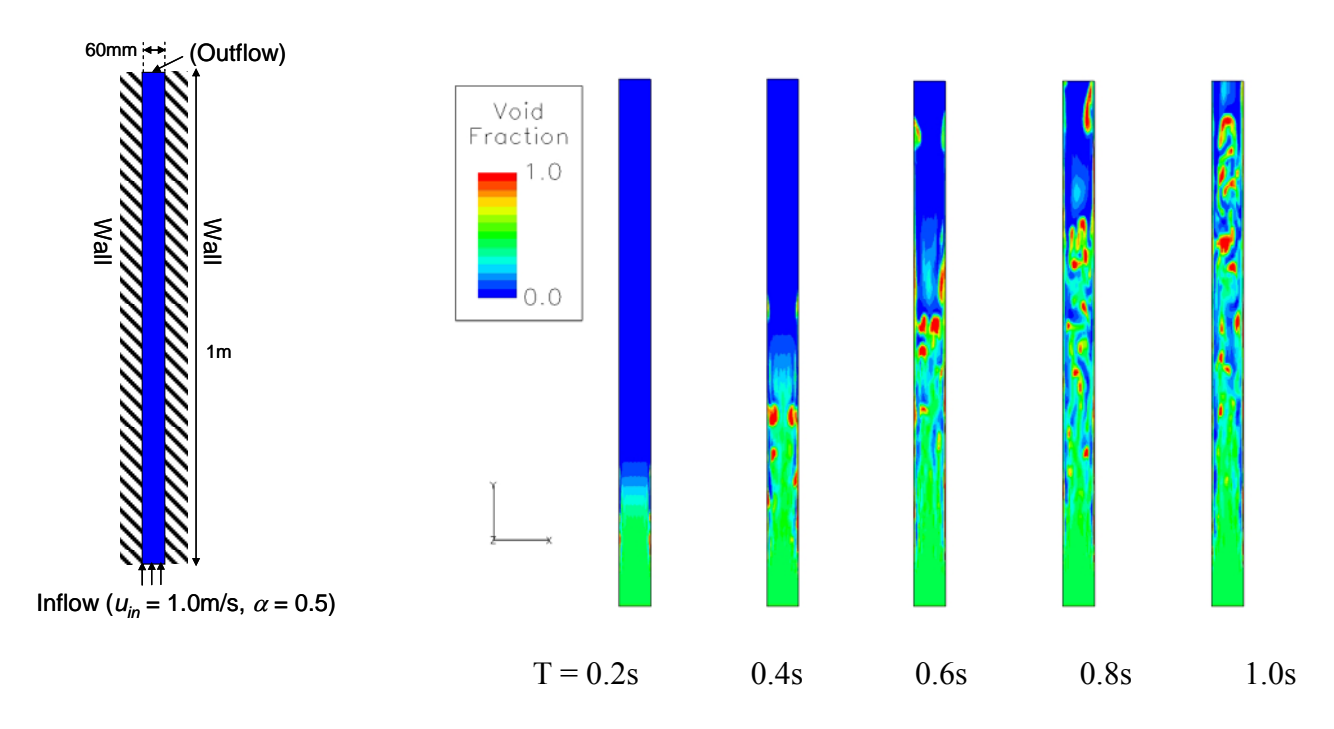


Figure 6 Computational domain.

Figure 7 Void fraction distribution.

## 2. Boiling simulation by phase-field model

# 2.1 Governing equations and numerical method

In this chapter, the boiling simulation for evaluating the thermal characteristic of two-phase flow is explained. To calculate the boiling bubble surface behaviour, the phase-field model is applied to our simulation method [9][10]. Governing equations for the boiling simulation are as bellows.

Mass conservation equation: 
$$\frac{\partial \rho}{\partial t} + \nabla \cdot (\rho \mathbf{u}) = 0$$
 (12)

Momentum conservation equation: 
$$\frac{\partial}{\partial t} (\rho \mathbf{u}) + \nabla \cdot (\rho \mathbf{u} \mathbf{u}) = -\nabla \cdot \mathbf{P} + \nabla \cdot \boldsymbol{\tau}$$
 (13)

Energy conservation equation:

$$\frac{\partial E}{\partial t} + \nabla \cdot (E\mathbf{u}) = \nabla \cdot [(-\mathbf{P} + \mathbf{\tau}) \cdot \mathbf{u}] + \nabla \cdot (k\nabla T) + \nabla \cdot [-\kappa_s \rho(\nabla \cdot \mathbf{u})\nabla \rho]$$
(14)

In above equations, the pressure tensor  $\mathbf{P}$ , the viscous stress tensor  $\mathbf{\tau}$ , and the total energy E are obtained by following equations,

$$\mathbf{P} = \left(p_0 - \kappa_s \rho \nabla^2 \rho - \frac{\kappa_s}{2} |\nabla \rho|^2\right) \mathbf{I} + \kappa_s \nabla \rho \otimes \nabla \rho, \qquad (15)$$

$$\boldsymbol{\tau} = \mu \left( \nabla \mathbf{u} + \nabla \mathbf{u}^T \right) - \frac{2}{3} \mu \left( \nabla \cdot \mathbf{u} \right) \mathbf{I} , \qquad (16)$$

$$E = \frac{1}{2}\rho|\mathbf{u}|^2 + e + \frac{\kappa_s}{2}|\nabla\rho|^2, \tag{17}$$

where  $p_0$  is the pressure in homogeneous system,  $\kappa_s$  is the surface tension parameter which controls the strength of the surface tension, and e is the internal energy. The governing equations were numerically solved by using the finite volume method and we used the "FrontFlow/red [8]" as the base program and the boiling analysis function was implemented. In this paper, the density for the steam phase and the water phase are calculated with using the JSME Steam Table [11]. The steamwater interface region is assumed to be the two-phase region, and the quality is solved from the local pressure and the enthalpy which are calculated by the above governing equations firstly. The two-phase specific volume can be solved by using the quality, the specific volume of the saturated steam and water. The two-phase density of the interface region can be given by the inverse of that specific volume.

#### 2.2 Results and discussions

In this section, the developed simulation method is applied to a three dimensional pool boiling problem and the numerical result is discussed. The computational domain is shown in Figure 8. The domain size is  $0.25[mm] \times 0.25[mm]$ , and divided into  $50 \times 50 \times 50$ . The top, side and

bottom boundaries are assumed to be the outlet, periodic and wall conditions respectively. In the centre of the bottom wall, the heated wall (iso-heat flux condition,  $q_{wall} = 200 [\text{kW/m}^2]$ ) is placed, and the other wall is the adiabatic condition. As initial condition, the static subcooled water is assumed, and initial pressure and temperature are 7.0[MPa] and 553.98[K].

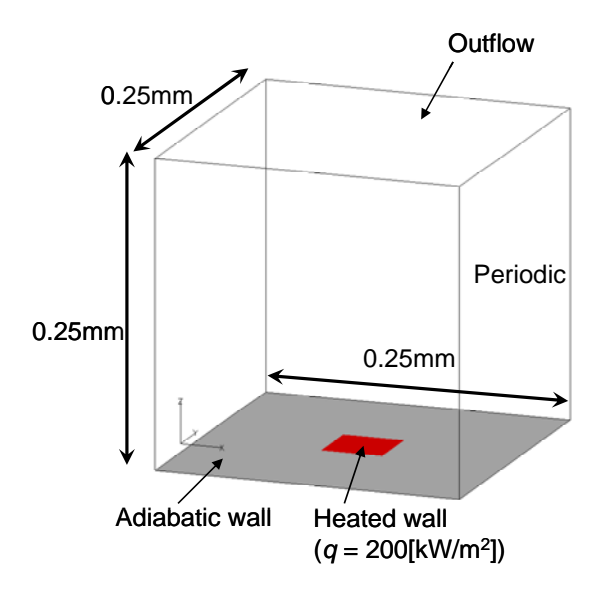


Figure 8 Computational domain and boundary conditions.

Figure 9 shows the numerical result with our developing simulation method. The upper, middle and lower figures represent the steam-water interface, the density distribution and the temperature distribution at each time. From Figure 9, it is recognized that the boiling bubble nucleates and grows on the heated wall, and departures from the wall when the bubble becomes sufficiently large. For this boiling process, the temperature inside the bubble becomes higher than the liquid phase, and the density inside the bubble can be kept small as the value of the steam (the saturated steam density is  $36.5[kg/m^3]$ ) by present method. However, from the density distribution, it is shown that the width of the diffusive interface region on the downstream of bubble becomes thicker than the upstream region caused by the wake flow of the rising bubble. Thus it is important that the numerical diffusion is reduced to track the steam-water interface and to predict the boiling process with high accuracy. The time variation of the average temperature on the heated wall is shown in Figure 10. Firstly, the wall temperature increases as the boiling bubble grows. When the bubble becomes large enough, the wall temperature begins to decrease. After that, the wall temperature begins to increase again. While increasing the wall temperature, the bubble departure from the wall is observed, and this process occurs periodically.

To evaluate the capability of the boiling analysis by the present method, the boiling heat transfer from our numerical result is compared to that given by the experimental correlation. The heat transfer coefficient for subcooled pool boiling is calculated according to the following Kutateladze's equation [12],

$$\frac{h_{boil}}{k_l} \sqrt{\frac{\sigma}{g(\rho_l - \rho_v)}} = 7.0 \times 10^{-4} Pr_l^{0.35} \left[ \frac{q}{\rho_v \Delta h \nu_l} \sqrt{\frac{\sigma}{g(\rho_l - \rho_v)}} \right]^{0.7} \left[ \frac{p}{\sigma} \sqrt{\frac{\sigma}{g(\rho_l - \rho_v)}} \right]^{0.7}$$
(18)

where  $h_{boil}$ ,  $k_l$ ,  $\rho_l$ ,  $\rho_v$ ,  $Pr_l$ ,  $\Delta h$  and  $v_l$  are the boiling heat transfer coefficient, thermal conductivity for water, water density, steam density, Prandtl number of water, latent heat and kinetic viscosity of water. The heat transfer coefficient  $h_{boil}$  obtained by Equation (18) is 40.7 [kW/m²/K] in this condition, and by our present method is  $4.6 \sim 7.7$  [kW/m²/K]. Thus  $h_{boil}$  for our method becomes one digit smaller than the value for the experimental correlation. For this reason, it is considered that the heated wall is assumed to be smoothly shaped and the small cavities on this wall are ignored for this simulation. Therefore the boiling bubble is difficult to be formed on the wall, and the wall temperature of simulation becomes higher than that of the experimental result. It seems to be the major problem of the present method to predict the effect of the surface on the boiling numerically.

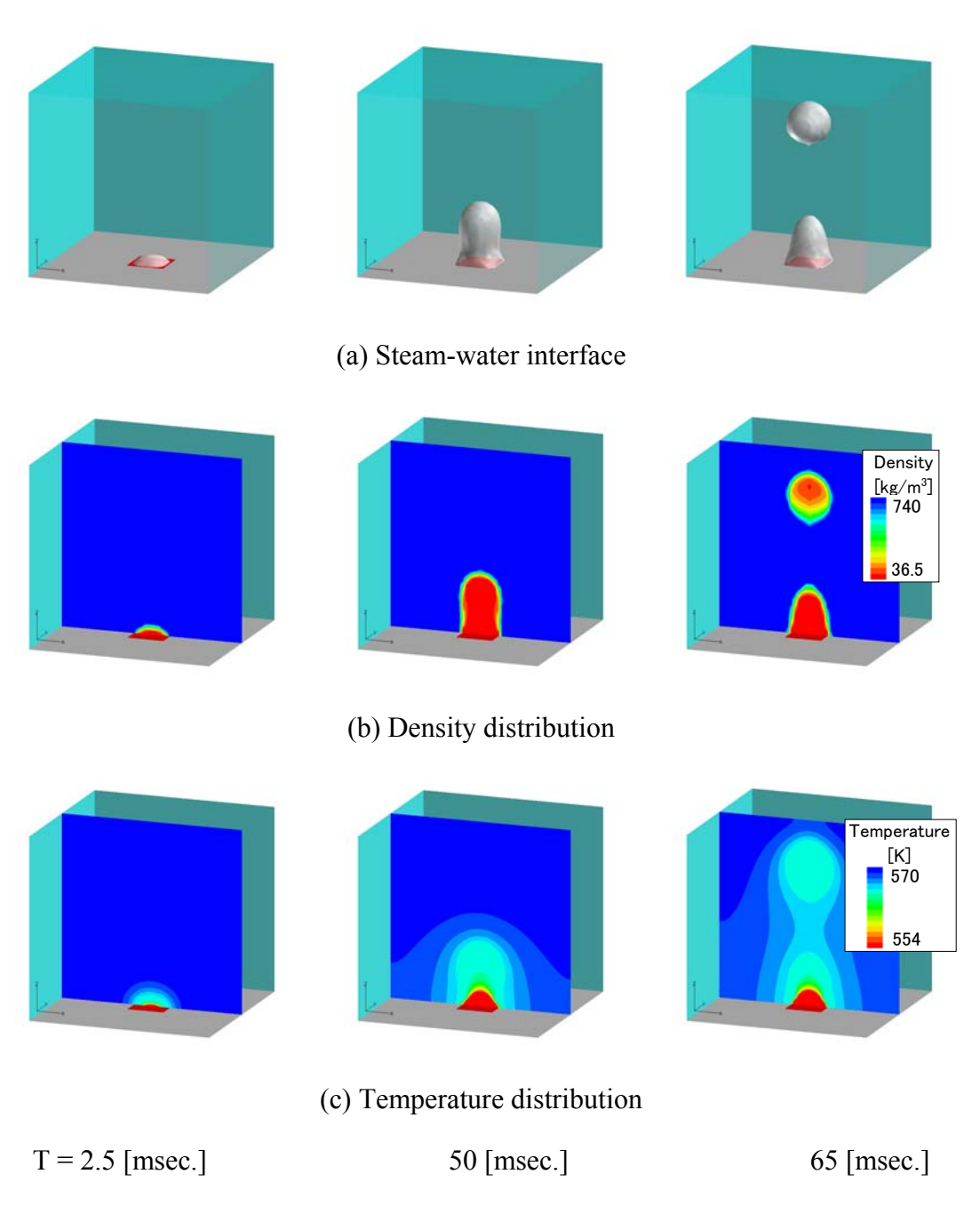


Figure 9 Numerical result of boiling bubble nucleation and departure from heated surface.

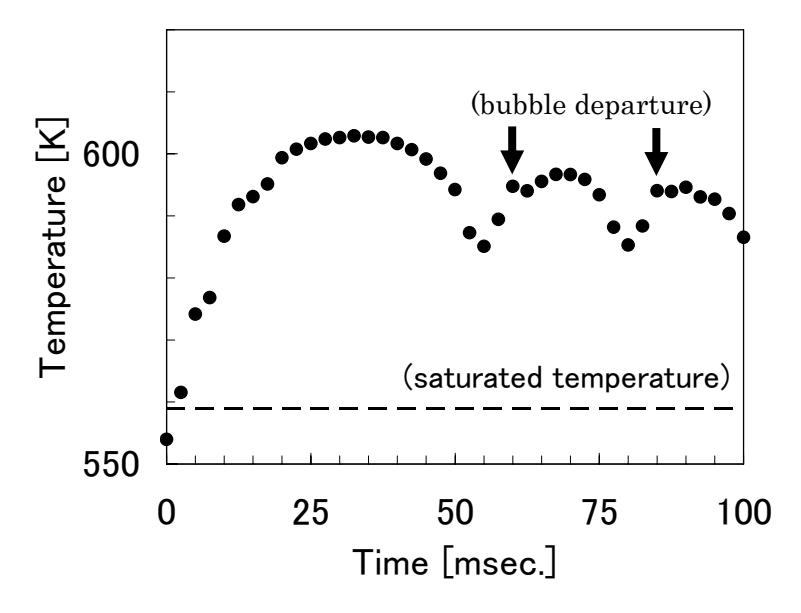


Figure 10 Average temperature of heated wall.

#### 3. Conclusion

In this paper, as part of the development of FDBA method, we have developed a numerical analysis method for evaluating the boiling two-phase flow in BWR fuel core. Firstly, to evaluate the two-phase flow transition, the hybrid two-phase flow analysis method was developed. We confirmed that the present method can simulate the various size bubbles behaviour simultaneously and the small bubbles coalescence into large bubbles, which causes the transition from the dispersed bubbly flow to the intermittent two-phase flow. Secondly, to simulate boiling phenomena, the phase-field model combined with Navier-Stokes equations was applied. For estimation of the thermodynamic properties of water and steam, we implemented the JSME Steam Table. By using the present method, a process of boiling bubbles nucleation, growth and departure from the heated wall can be simulated. We confirmed that it is possible to simulate the boiling phenomena such as boiling heat transfer by numerical analysis directly. For application of the two-phase CFD model to the FDBA method, the additional study is necessary to improve the prediction accuracy of boiling two-phase flow phenomena.

### 4. References

- Y. Yamamoto and T. Mitsutake, "New design procedure development of future reactor critical power estimation (1) Practical design-by-analysis method for BWR critical power design correlation", Proceedings of the 15<sup>th</sup> International Conference on Nuclear Engineering, Nagoya, Japan, 2007 April 22-26.
- [2] Y. Yamamoto and T. Mitsutake, "Design-by-analysis application to next generation BWR fuel thermal design method", <u>Proceedings of the 6<sup>th</sup> Japan-Korea Symposium on Nuclear Thermal</u> Hydraulic and Safety, Okinawa, Japan, 2008, November 24-27.

- [3] A. Minato, T. Nagayoshi, M. Misawa, A. Suzuki, H. Ninokata and S. Koshizuka, "Numerical Simulation Method of Complex 3D Gas-Liquid Two-Phase Flow", <u>Proceedings of the 5<sup>th</sup> International Conference on Multiphase Flow</u>, Yokohama, Japan, 2004 May 30 June 4.
- [4] K. Sakoda, A. Sou and A. Tomiyama, "A hybrid method for predicting dispersed gas-liquid and liquid-liquid multi-phase flows", Progress in multiphase flow research I, 2006. pp. 163-170 (in Japanese).
- [5] CD-adapco, "Methodology, STAR-CD version 3.26," 2005.
- [6] T. R. Auton, "The lift force on a spherical body in a rotational flow", Journal of Fluid Mechanics, Vol. 183, 1987, pp. 199-218.
- [7] J. U. Brackbill, D. B. Kothe and C. Zemach, "A Continuum Method for Modeling Surface Tension", Journal of Computational Physics, Vol. 100, No. 2, 1992, pp. 335-354.
- [8] Center for Research on Innovative Simulation Software, http://www.ciss.iis.u-tokyo.ac.jp/english/index.php.
- [9] N. Takada, M. Misawa and A. Tomiyama, "A phase-field method for interface-tracking simulation of two-phase flows", <u>Proceedings of 2005 ASME Fluids Engineering Division Summer Meeting and Exhibition</u>, Houston, TX, USA, 2005, June 19-23.
- [10] T. Seta and K. Okui, "The single component thermal lattice Boltzmann simulation of pool boiling in two dimensions", Journal of Thermal Science and Technology, Vol. 1, No. 2, 2006, pp. 125-137.
- [11] "JSME Steam Tables", The Japan Society of Mechanical Engineering, 1999.
- [12] "JSME Data Book: Heat Transfer 4<sup>th</sup> Edition", The Japan Society of Mechanical Engineering, 1986.